

High Order Perturbation Theory for Helmholtz/Schrödinger Equations via a Separable Preconditioner

Åke Edlund,* Ilya Vorobeichik,† and Uri Peskin‡¹

Department of Chemistry, Technion-Israel Institute of Technology, Haifa 32000, Israel
E-mail: *ake@tdb.uu.se; †chrilya, ‡uri@chem.technion.ac.il

Received April 22, 1997; revised September 11, 1997

A numerical procedure is suggested for the solution of multidimensional inhomogeneous Helmholtz/Schrödinger equations. The procedure is based on coordinate-space (grid) representations in which all the coupling terms (\hat{V}) between different degrees of freedom are local (diagonal) and therefore the remaining differential (nonlocal) terms are separable. This separability leads to an efficient (sparse) representation of an approximate Green's operator (\hat{G}_0). For sufficiently "weak" coupling, a low order expansion in powers of $\hat{G}_0 \hat{V}$ provides the solution according to Rayleigh Schrödinger perturbation theory. For "strong" coupling intensities the sparse structure of \hat{G}_0 makes it an efficient preconditioner for high order iterative solutions (e.g., the QMR algorithm of Freund and Nachtigal). The high order power expansion in $\hat{G}_0 \hat{V}$ provides an optimized perturbative series which converges for strong coupling intensities. A numerical example is given for the Helmholtz equation in three dimensions. © 1997 Academic Press

I. INTRODUCTION

The solution of *inhomogeneous wave equations* of the type

$$\hat{A}\chi = \phi, \tag{1.1}$$

where \hat{A} is a second-order, regular partial (multidimensional) differential operator is common in numerical simulations of physical and chemical systems [1, 2]. In

¹ Corresponding author.

some cases the inhomogeneous term is intrinsic to the equation (e.g., in the Poisson equation for the electrostatic potential). In other cases, the inhomogeneous term is introduced in order to impose specific boundary conditions (a current source [3]) on the solution of *homogeneous* wave equations, such as Laplace, Helmholtz, or Schrödinger equations (see, for example, Refs. [4–14] for applications). In general, the solution to the inhomogeneous equation (1.1) is the Green’s function for the corresponding homogeneous equation when ϕ is chosen as a delta function in the coordinate representation [2].

Unfortunately, already in three dimensions (corresponding, e.g., to a Cartesian coordinate space) the discrete representation of the differential operator \hat{A} may become too large to allow its storage in full dimensionality, and direct inversion methods for solving Eq. (1.1) become impractical. The solution in these cases is limited to iterative schemes.

The simplest iterative approach to wave equations is Rayleigh Schrödinger perturbation theory [15, 16], which is based on splitting \hat{A} into a zero-order approximation \hat{A}_0 and a perturbation \hat{V} so that

$$\hat{A} = \hat{A}_0 - \hat{V}. \tag{1.2}$$

The formal solution to Eq. (1.1) is

$$\chi = \hat{G} \phi, \tag{1.3}$$

where \hat{G} is the inverse (Green’s) operator

$$\hat{G} = \hat{A}^{-1}. \tag{1.4}$$

An approximate solution can be obtained by the truncated perturbative expansion (the Born series),

$$\hat{G} = \hat{G}_0 + \hat{G}_0 \hat{V} \hat{G}_0 + \hat{G}_0 \hat{V} \hat{G}_0 \hat{V} \hat{G}_0, + \dots, \tag{1.5}$$

in which the zero-order Green’s operator is defined as

$$\hat{G}_0 = \hat{A}_0^{-1}. \tag{1.6}$$

This approach is useful as long as \hat{A}_0 is sufficiently close to \hat{A} , or alternatively, when \hat{V} is a sufficiently “small” perturbation [15, 16]. In such cases, a low order expansion converges to the correct solution. However, the perturbative series diverges for “large” \hat{V} which is a severe limitation in many applications of practical interest (see, for example, the numerical example below).

An alternative to perturbation theory is to solve Eq. (1.1) by high-order iterative (Krylov subspace based) methods [17–22]. The approximation after k iterations reads

$$\chi^k = \sum_{j=0}^k \alpha_{j,k} \hat{A}^j \phi, \tag{1.7}$$

where $\{\alpha_{j,k}\}$ are optimized expansion coefficients which minimize the residual vector $\chi - \chi^k$. Important progress has been made recently in the development of these approaches for the general case of *non-Hermitian* linear systems. (In particular, we refer to the quasi minimal residual (QMR) algorithm of Freund and Nachtigal [23, 24]). However, a successful implementation of the method usually requires an efficient preconditioner [19] which minimizes the number of iterations.

Below we present an optimized high-order iterative solution of Helmholtz/Schrödinger equations, based on an approximate Green's operator \hat{G}_0 as an efficient preconditioner. The equation is represented in a discrete coordinate (grid) space [25–28] in which the coupling \hat{V} is diagonal (local) and therefore the nondiagonal (nonlocal) term, \hat{A}_0 , is separable in the different degrees of freedom. This structure leads to a sparse representation of \hat{G}_0 which is similar to that of the Fourier grid preconditioner as described in Ref. [8], but which applies also when the separable term contains mixed local and differential operators. The combination of a sparse \hat{G}_0 and a diagonal \hat{V} provides an efficient high-order iterative expansion (using the QMR algorithm) in powers of $\hat{G}_0 \hat{V}$ which converges in cases where the perturbative expansion diverges.

In Section II the simple relation between the perturbative series expansion and iterative Krylov subspace-based methods is given for clarity. The sparse preconditioner is introduced in Section III and an illustrative numerical application to the solution of the Helmholtz equation in three dimensions is given in Section IV. Conclusions are given in Section V.

II. AN OPTIMIZED HIGH-ORDER PERTURBATION THEORY

An alternative approach to the perturbative series expansion is to apply the approximate Green's operator \hat{G}_0 as a preconditioner to Eq. (1.1) and to solve the equation by standard Krylov subspace-based iterative methods [17–22]. The general approach is to replace Eq. (1.1) by

$$\hat{G}_0 \hat{A} \chi = \hat{G}_0 \phi. \quad (2.1)$$

Using Eq. (1.2) one obtains

$$(\hat{I} - \hat{G}_0 \hat{V}) \chi = \hat{G}_0 \phi. \quad (2.2)$$

For sufficiently small $\hat{G}_0 \hat{V}$ (more precisely, when the spectrum of $\hat{G}_0 \hat{V}$ in a discrete representation is within the unit circle [17, 18]) the perturbative expansion (Eq. (1.5)) is the formal solution to Eq. (2.2),

$$\chi = \frac{1}{\hat{I} - \hat{G}_0 \hat{V}} \hat{G}_0 \phi = \sum_{j=0}^{\infty} (\hat{G}_0 \hat{V})^j \hat{G}_0 \phi. \quad (2.3)$$

However, Eq. (2.2) can be solved even for “large” $\hat{G}_0\hat{V}$ by construction of a converging set of approximate solutions in the span of the Krylov subspace $K[(\hat{I} - \hat{G}_0\hat{V}), \hat{G}_0\phi]$, where the k th approximation is given by

$$\chi^k = \sum_{j=0}^k \alpha_{j,k} (\hat{I} - \hat{G}_0\hat{V})^j \hat{G}_0\phi = \sum_{j=0}^k \beta_{j,k} (\hat{G}_0\hat{V})^j \hat{G}_0\phi. \tag{2.4}$$

The number of iterations required for convergence is minimized when \hat{G}_0 is a good approximation to \hat{A}^{-1} , i.e. when \hat{V} is small. However, unlike in the perturbative expansion, convergence will be obtained even for “large” \hat{V} since the expansion coefficients $\{\beta_{j,k}\}$ (which are set to unity in the Born expansion) are optimized and adjusted in order to minimize the residual vector $(\chi^k - \chi)$. Nevertheless, the resulting scheme is a high-order procedure, requiring large numbers of $\hat{G}_0\hat{V}$ operations which may make the scheme impractical. In exact arithmetics the Krylov subspace approximation is *guaranteed* to converge only when the number of iterations approaches the size of the matrix representation of \hat{A} , which may become very large (e.g., 10^5 – 10^6 in the example given below). An efficient preconditioner \hat{G}_0 is therefore of major importance.

III. THE SPARSE SEPARABLE PRECONDITIONER

As described above, the main numerical effort in the high-order iterative scheme is associate with the successive operations of $\hat{G}_0\hat{V}$. We therefore search for an efficient representation in which $\hat{G}_0\hat{V}$ is “economical.” Our strategy is based on choosing a discrete representation of the Helmholtz/Schrödinger equation in which the coupling between different degrees of freedom is diagonal. A discrete coordinate (grid) representation is a natural choice for that matter since the physical coupling terms are often local (e.g., the interaction potential in quantum mechanics, or the refractive index distribution in optics are diagonal in a Cartesian coordinate system representation). The nonlocal (differential) operators are nondiagonal in the coordinate representation [25–28]. However, since the coupling terms are diagonal the nondiagonal terms are separable in the different degrees of freedom. The resulting generic structure of \hat{A} for n coupled degrees in this representation takes the form

$$\hat{A} = \sum_{l=1}^n \hat{A}_l - \hat{V}, \tag{3.1}$$

where \hat{V} is a diagonal n -dimensional coupling operator,

$$\hat{V} \equiv \nu^d, \tag{3.2}$$

and each operator \hat{A}_l ($l = 1, \dots, n$) is unity with respect to all but the l th degree of freedom. The matrix representation of \hat{A}_l is defined as

$$\hat{A}_l \equiv \mathcal{A}_l, \tag{3.3}$$

where

$$\mathcal{A}_l = \mathbf{I}_1 \otimes \mathbf{I}_2 \otimes \cdots \otimes \mathbf{I}_{l-1} \otimes \mathbf{A}_l \otimes \mathbf{I}_{l+1} \otimes \cdots \otimes \mathbf{I}_n. \quad (3.4)$$

\mathbf{I}_l is an $N_l \times N_l$ identity matrix and \mathbf{A}_l is an $N_l \times N_l$ nondiagonal matrix representation of an operator in the subspace of the l th degree of freedom. Equation (1.1) can be rewritten in matrix form,

$$\left(\sum_{l=1}^n \mathcal{A}_l - \boldsymbol{\nu}^d \right) \boldsymbol{\chi} = \boldsymbol{\phi}, \quad (3.5)$$

where $\boldsymbol{\chi}$ and $\boldsymbol{\phi}$ are $\mathcal{N} = \prod_{l=1}^n N_l$ -dimensional vectors. As one can see, a matrix vector multiplication of $\sum_{l=1}^n \mathcal{A}_l - \boldsymbol{\nu}^d$ requires $\mathcal{N} \times (1 + \sum_{l=1}^n N_l)$ scalar multiplications, which is much smaller than the matrix dimension \mathcal{N}^2 . Therefore, Eq. (3.5) is a very *sparse* linear system.

The preconditioner for Eq. (3.5) is chosen as the inverse of the separable operator \hat{A}_0 ,

$$\mathcal{G}_0 = \mathcal{A}_0^{-1} = \left(\sum_{l=1}^n \mathcal{A}_l \right)^{-1}, \quad (3.6)$$

and the preconditioned system reads

$$(\mathcal{I} - \mathcal{G}_0 \boldsymbol{\nu}^d) \boldsymbol{\chi} = \mathcal{G}_0 \boldsymbol{\phi}. \quad (3.7)$$

While \hat{A}_0 is a separable approximation to \hat{A} , its inverse \hat{G}_0 is clearly not separable, and therefore *the matrix \mathcal{G}_0 is dense and impractical for the iterative scheme. However, the separability of \hat{A}_0 can be used in order to represent \mathcal{G}_0 as a sequence of sparse matrix multiplications as*

$$\mathcal{G}_0 = \mathcal{U}_R (\boldsymbol{\lambda}^d)^{-1} \mathcal{U}_L, \quad (3.8)$$

where $\boldsymbol{\lambda}^d$ is the diagonal eigenvalues matrix of \mathcal{A}_0 ,

$$\mathcal{A}_0 \mathcal{U}_R = \mathcal{U}_R \boldsymbol{\lambda}^d, \quad (3.9)$$

$$\mathcal{U}_L = \mathcal{U}_R^{-1}. \quad (3.10)$$

(Note that, in general (for non-Hermitian \mathcal{A}_0), the existence of Eq. (3.8) is not guaranteed. We shall therefore limit the discussion only to cases in which Eq. (3.8) is valid.) The first operation \mathcal{U}_L onto a vector is a transformation to the basis in which \mathcal{A}_0 is diagonal. Since \mathcal{A}_0 is separable, this transformation can be carried out in successive steps,

$$\mathcal{U}_L = \mathcal{U}_{L_1} \mathcal{U}_{L_2} \mathcal{U}_{L_3} \cdots \mathcal{U}_{L_n}, \quad (3.11)$$

where each step involves a sparse matrix multiplication

$$\mathcal{U}_{L_l} = \mathbf{I}_1 \otimes \mathbf{I}_2 \otimes \cdots \otimes \mathbf{I}_{l-1} \otimes \mathcal{U}_l \otimes \mathbf{I}_{l+1} \otimes \cdots \otimes \mathbf{I}_n. \tag{3.12}$$

and the (small) matrices $\{\mathbf{U}_l\}$ are the diagonalization matrices in the subspaces of the different degrees of freedom, i.e.,

$$\mathbf{U}_l \mathbf{A}_l \mathbf{U}_l^{-1} = \Lambda_l^d. \tag{3.13}$$

The second operation is the *diagonal inversion* $(\boldsymbol{\lambda}^d)^{-1}$. Note that while $\boldsymbol{\lambda}^d$ is separable in the different degrees of freedom,

$$\boldsymbol{\lambda}^d = \sum_{l=1}^n \mathbf{I}_1 \otimes \mathbf{I}_2 \otimes \cdots \otimes \mathbf{I}_{l-1} \otimes \Lambda_l^d \otimes \mathbf{I}_{l+1} \otimes \cdots \otimes \mathbf{I}_n; \tag{3.14}$$

its inverse is a diagonal coupling matrix. The third operation is the back transformation into the original matrix representation,

$$\mathcal{U}_R = \mathcal{U}_{R_1} \mathcal{U}_{R_2} \mathcal{U}_{R_3} \cdots \mathcal{U}_{R_n}, \tag{3.15}$$

which, again, involves only sparse matrix multiplications,

$$\mathcal{U}_{R_l} = \mathcal{U}_{L_l}^{-1} = \mathbf{I}_1 \otimes \mathbf{I}_2 \otimes \cdots \otimes \mathbf{I}_{l-1} \otimes \mathcal{U}_l^{-1} \otimes \mathbf{I}_{l+1} \otimes \cdots \otimes \mathbf{I}_n. \tag{3.16}$$

According to Eqs. (3.11), (3.12), the number of scalar multiplications in applying \mathcal{U}_L is $\mathcal{N} \times \sum_{l=1}^n N_l$ and similarly for \mathcal{U}_R . Neglecting the (order \mathcal{N}) diagonal operation $(\boldsymbol{\lambda}^d)^{-1}$, we find that applying \mathcal{G}_0 requires only twice the number of scalar multiplications in comparison to applying \mathcal{A}_0 . Thus we were able to make use of the separability of \hat{A}_0 in order to apply its nonseparable inverse \hat{G}_0 using only sparse representations.

IV. NUMERICAL EXAMPLE

As a model problem we consider the light distribution near a defect in a rectangular waveguide, as obtained from the solution of the Helmholtz equation in three dimensions when polarization effects are neglected. (This problem is analogous to the scattering of quantum particles of an obstacle within a two-dimensional rectangular tube, as described by the solution of the Schrödinger equation.) The stationary Helmholtz equation [3, 14, 29] takes the form of Eq. (1.1), where the three-dimensional differential operator reads

$$\hat{A}_{x,y,z} \equiv \nabla_x^2 + \nabla_y^2 + \nabla_z^2 + k^2 n^2(x, y, z) + i \varepsilon(x, y, z). \tag{4.1}$$

$k = 2\pi/1.5$ is the free space wave vector, $n(x, y, z)$ is the index of refraction distribution, and the imaginary term $i \varepsilon(x, y, z)$ is introduced in order to impose the proper scattering boundary conditions on the wave function [4, 5, 14]. The

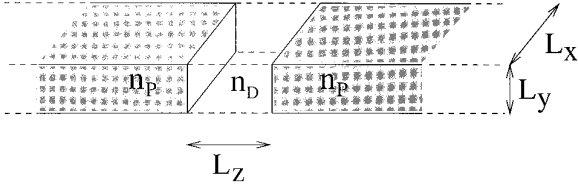


FIG. 1. A discontinuous rectangular waveguide.

geometry of the rectangular waveguide with lateral metal coating is plotted in Fig. 1. The corresponding index of refraction distribution is given by

$$n^2(x, y, z) = n_p^2(x, y, z) + n_D^2(x, y, z), \tag{4.2}$$

where n_p and n_D correspond to the “perfect” and “defected” areas, respectively,

$$n_p^2(x, y, z) = \begin{cases} n_{p_x}^2(x) + n_{p_y}^2(y), & |z| > \frac{L_z}{2}, \\ 0 & |z| \leq \frac{L_z}{2}; \end{cases} \tag{4.3}$$

$$n_D^2(x, y, z) = \begin{cases} n_{D_x}^2(x) + n_{D_y}^2(y), & |z| \leq \frac{L_z}{2}, \\ 0 & |z| > \frac{L_z}{2}. \end{cases}$$

The lateral waveguide profiles are modeled as

$$n_{p_x}(x) = \begin{cases} \frac{n_{p0}}{\sqrt{2}} |x| < L_x/2, \\ \frac{n_{p1}}{\sqrt{2}} |x| \geq L_x/2; \end{cases}$$

$$n_{p_y}(y) = \begin{cases} \frac{n_{p0}}{\sqrt{2}} |y| \geq L_y/2, \\ \frac{n_{p1}}{\sqrt{2}} |y| \leq L_x/2; \end{cases} \tag{4.4}$$

$$n_{D_x}(x) = \begin{cases} \frac{n_{D0}}{\sqrt{2}} |x| < L_x/2, \\ \frac{n_{D1}}{\sqrt{2}} |x| \geq L_x/2; \end{cases}$$

$$n_{D_y}(y) = \begin{cases} \frac{n_{D0}}{\sqrt{2}} |y| \geq L_y/2, \\ \frac{n_{D1}}{\sqrt{2}} |y| \leq L_x/2; \end{cases}$$

$n_{p0} = 1.5$ and $n_{p1} = i1000$ are the internal (glass) and external (metal coating) refraction indexes of the perfect waveguide (absorption of the coating is neglected). The defect is characterized by the internal and external indexes n_{D0} and n_{D1} . The imaginary function $i \varepsilon(x, y, z)$ vanishes, except at the boundaries of the numerical grid, and it is given by

$$\varepsilon(x, y, z) = \varepsilon_{+x}(x) + \varepsilon_{-x}(x) + \varepsilon_{+y}(y) + \varepsilon_{-y}(y) + \varepsilon_{+z}(z) + \varepsilon_{-z}(z), \quad (4.5)$$

where, for example,

$$\varepsilon_{+z}(z) = \begin{cases} h_z \left(\frac{z - z_0}{Z/2 - z_0} \right)^4, & z \geq z_0, \\ 0 & , \quad z < z_0, \end{cases} \quad (4.6)$$

$$\varepsilon_{-z}(z) = \varepsilon_{+z}(-z),$$

and similarly for $\varepsilon_{\pm y}(y)$ and $\varepsilon_{\pm x}(x)$.

The incoming radiation flux (in the positive direction of the z axis) was chosen as the fundamental lateral mode of the rectangular waveguide, characterized by the propagation constant $\beta = 5.1540 \mu\text{m}^{-1}$,

$$\varphi(x, y, z) = \sqrt{\frac{2}{L_x}} \sin\left(\frac{\pi(x + L_x/2)}{L_x}\right) \sqrt{\frac{2}{L_y}} \sin\left(\frac{\pi(y + L_y/2)}{L_y}\right) \sqrt{\frac{1}{2\beta}} e^{i\beta z}. \quad (4.7)$$

These incoming wave boundary conditions are imposed implicitly within the inhomogeneous (right-hand side) term,

$$\phi \equiv i\varepsilon_{-z}(z)\varphi(x, y, z). \quad (4.8)$$

Substitution of Eqs. (4.1)–(4.8) into Eq. (1.1) defines the inhomogeneous scalar wave equation for the light distribution. The different propagation directions (x, y, z) are coupled via the index of refraction distribution $n^2(x, y, z)$. A diagonal matrix representation is chosen for this operator; i.e., $n^2(x, y, z)$ and $\varepsilon(x, y, z)$ are sampled on a three-dimensional discrete grid, $n^2(x_i, y_j, z_k)$ and $\varepsilon(x_i, y_j, z_k)$, where

$$x_i = -\frac{X}{2} + (i - 1)X/(N_x - 1), \quad i = 1, 2, \dots, N_x,$$

$$y_j = -\frac{Y}{2} + (j - 1)Y/(N_y - 1), \quad j = 1, 2, \dots, N_y, \quad (4.9)$$

$$z_k = -\frac{Z}{2} + (k - 1)Z/(N_z - 1), \quad k = 1, 2, \dots, N_z,$$

and (i, j, k) corresponds to a point in an $N_x \times N_y \times N_z$ -dimensional discrete space. The second derivative operators are nondiagonal. The discrete variable representation of these operator is given by [28]

$$\{\nabla_x^2\}_{(i,j,k),(i',j',k')} = \delta_{j,j'}\delta_{k,k'} \begin{cases} \frac{-\pi^2 N_x^2}{3X^2}, & i = i', \\ \frac{-2N_x^2(-1)^{i-i'}}{(i-i')X^2}, & i \neq i', \end{cases} \tag{4.10}$$

and similarly for ∇_y^2 and ∇_z^2 .

As a preconditioner we chose a separable approximation to the matrix representation of $\hat{A}_{x,y,z}$ which represents the perfect (defect-free) waveguide. I.e.,

$$\mathcal{A}_0 = \mathcal{A}_x + \mathcal{A}_y + \mathcal{A}_z, \tag{4.11}$$

where

$$\begin{aligned} \mathcal{A}_x &= [\nabla_x^2 + k^2 n_{px}^2(x) + i(\epsilon_{+x}(x) + \epsilon_{-x}(x))] \otimes \mathbf{I}_{N_y} \otimes \mathbf{I}_{N_z}, \\ \mathcal{A}_y &= \mathbf{I}_{N_x} \otimes [\nabla_y^2 + k^2 n_{py}^2(y) + i(\epsilon_{+y}(y) + \epsilon_{-y}(y))] \otimes \mathbf{I}_{N_z}, \\ \mathcal{A}_z &= \mathbf{I}_{N_x} \otimes \mathbf{I}_{N_y} \otimes [\nabla_z^2 + i(\epsilon_{+z}(z) + \epsilon_{-z}(z))]. \end{aligned} \tag{4.12}$$

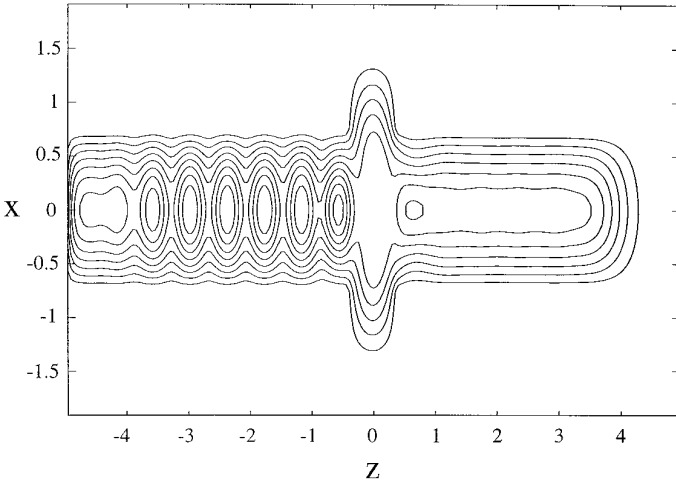


FIG. 2. A contour plot of the light intensity in the (x, z) plane (at $y = 0.0 \mu\text{m}$) near the waveguide discontinuity. The computational parameters are (see Eqs. (4.3), (4.4), (4.6), (4.9) for definitions) $L_x = 1.5$, $L_y = 1.0$, and $L_z = 0.8$; 405,000 grid points were used to represent the wave function ($N_x = 45$, $N_y = 45$, $N_z = 200$), $X = 4.0$, $Y = 3.0$, $Z = 10.0$, $h_x = h_y = h_z = 200$, $x_0 = 1.0$, $y_0 = 0.7$, $z_0 = 2.5$ (all length units are in μm). The results are converged with respect to the grid density. The wavefunction is damped near the grid boundaries due to the imaginary boundary operators.

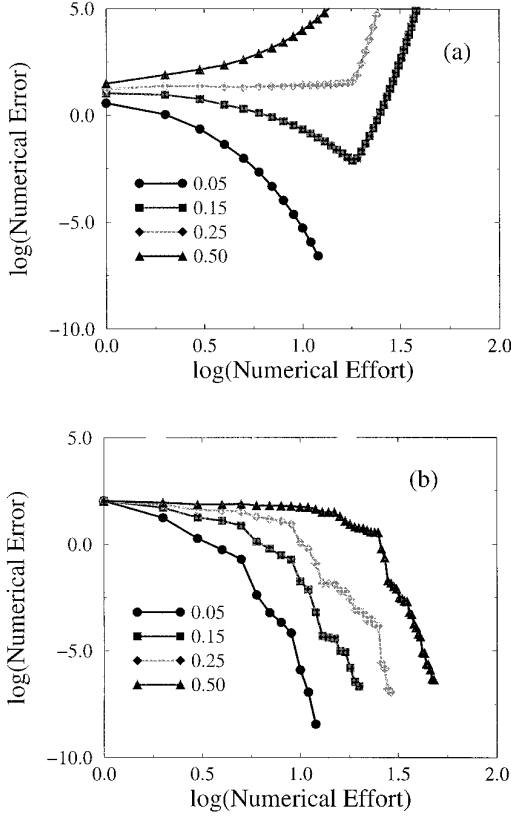


FIG. 3. A log–log plot of the numerical error versus the numerical effort in calculating the wavefunction in the defect area. The error is defined as the norm of the residual vector, $|\phi - \mathcal{A}\chi|$, and the numerical effort is measured in units of $\mathcal{S}_0 \nu^d$ operations: (a) perturbation theory (Eq. (2.3)); (b) optimized perturbation expansion (Eq. (2.4)). The results are given for increasing perturbation intensities in the defect area, $n_{p0} - n_{D0} = 0.05, 0.15, 0.25, 0.5$. The computational parameters are $L_x = 1.5, L_y = 1.0, L_z = 2.0, N_x = 30, N_y = 30, N_z = 100, X = 4.0, Y = 3.0, Z = 10.0, h_x = h_y = 0, h_z = 200, x_0 = 1.0, y_0 = 0.7, z_0 = 2.5$ (all length units are in μm).

The nonseparable (coupling) term is, therefore,

$$\nu^d = \mathcal{A}_0 - \mathcal{A}. \tag{4.13}$$

ν^d is the diagonal matrix which represents the difference in the refractive index distribution between the perfect and the defected waveguides. The light distribution (χ) was obtained by solving Eq. (3.7) using the optimized perturbation expansion as described above with $\mathcal{S}_0 = \mathcal{A}_0^{-1}$. The quasi minimal residual (QMR) algorithm (for details see Refs. [23, 24]) was used in order to optimize the expansion coefficients.

A two-dimensional cut through the three-dimensional wavefunction around the defect area is plotted in Fig. 2. The defect represents a discontinuity of the wave

guide along the z axis (see Fig. 1) in which the light propagates in vacuum, i.e. $n_{D0} = n_{D1} = 1$. This discontinuity is shown to reflect some of the incoming radiation flux on expense of the transmission efficiency. Moreover, the longitudinal propagation is shown to be strongly coupled to the lateral dimensions, resulting in radiation leak outside the waveguide. (The latter phenomena is pronounced since the lateral dimensions $L_x = 1.5 \mu m$ and $L_y = 1.0 \mu m$ are of the order of the radiation wavelength $\lambda = 1.5 \mu m$.)

To illustrate the advantage of the optimal perturbation expansion with respect to the standard perturbation theory, we need to address a simpler case for which both approaches are comparable. We consider a waveguide with a discontinuous *internal* refraction index, but with a perfect coating, so that $n_{D1} = n_{P1}$. The perturbation induced by the defect increases as the internal refraction index changes from $n_{D0} = 1.5$ (perfect waveguide) to $n_{D0} = 1.0$ (the vacuum value). Fig. 3a illustrates the breakdown of the standard perturbation theory, which fails to converge for large deviations between the defect and the perfect refraction indexes. On the other hand, when the expansion coefficients are optimized (in this case, by the QMR algorithm) the series converges regardless of the value of n_{D0} as illustrated in Fig. 3b. In Fig. 4 we compare the optimized solutions of the original equation (Eq. (1.7)) and the preconditioned system (Eq. (2.4)). It is seen that although the iterative algorithm (QMR) converges for both representations, a significant (in this case two orders of magnitude) reduction in the number of iterations is obtained when \mathcal{S}_0 is applied as a preconditioner. This is translated directly to a significant reduction in the numerical effort, since the sparse matrix multiplications of \mathcal{S}_0 require only twice the effort of applying \mathcal{A} directly. We therefore demonstrated that it is the combination of an efficient sparse preconditioner with optimized expansion coefficients which makes the approach powerful.

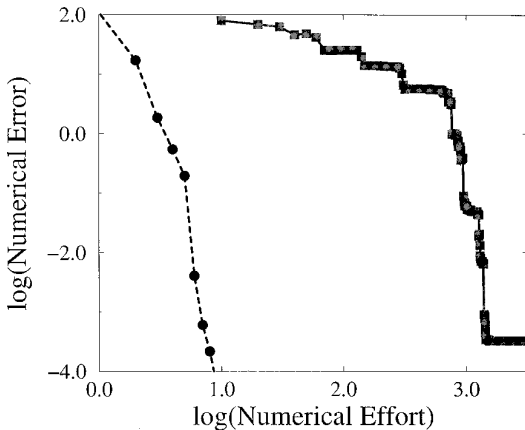


FIG. 4. A log–log plot of the numerical error versus the numerical effort in calculating the wavefunction in the defect area. The error is defined as the norm of the residual vector, $|\phi - \mathcal{A}\chi|$, and the numerical effort is measured in units of QMR iterations: solid, the original equation (Eq. (3.5)); dashed, the preconditioned system (Eq. (3.7)). The perturbation is characterized by $n_{P0} - n_{D0} = 0.05$. The other computational parameters are the same as in Fig. 3.

V. CONCLUSIONS

An efficient high-order perturbation expansion for multidimensional inhomogeneous Helmholtz/Schrödinger equations with local (diagonal) coupling was presented. The procedure involves an efficient sparse preconditioner (approximate Green's operator) within a Krylov iterative method (QMR). Unlike in perturbation theory the high-order expansion is not limited to small perturbations and enables treatments of systems in which the nonseparability is pronounced. The present procedure is limited, however, to matrix representations of the wave equation in which the coupling between different degrees of freedom is diagonal. Generalizations of the separable preconditioner scheme to systems with nondiagonal (but sparse) coupling, as well as comparisons of the sparse preconditioner to other standard preconditioners are in progress and are beyond the scope of the present work.

ACKNOWLEDGMENTS

U. P. is an Yigal Alon Fellow and a Theodore and Mina Bergman academic lecturer. This research was supported by the foundation for promotion of research at the Technion, by the I. Goldberg fund for electronics research and by the Israel Science Ministry. Å. E. was supported by the Göran Gustafsson foundation.

REFERENCES

1. S. E. Koonin and D. C. Meredith, *Computational Physics* (Addison-Wesley, Reading, MA, 1990).
2. C. W. Wong, *Introduction to Mathematical Physics* (Oxford, New York, 1991).
3. A. W. Snyder and J. D. Love, *Optical Waveguide Theory* (Chapman & Hall, New York, 1983).
4. D. Neuhauser, State-to-state reactive scattering amplitudes from single-arrangement propagation with absorbing potentials, *Chem. Phys. Lett.* **200**, 7836 (1990).
5. T. Seideman and W. H. Miller, Calculation of the cumulative reaction probability via a discrete representation with absorbing boundary conditions, *J. Chem. Phys.* **96**, 4412 (1992).
6. W. H. Thompson and W. H. Miller, State-specific reaction probabilities from a DVR-ABC Green function, *Chem. Phys. Lett.* **206**, 123 (1993).
7. V. A. Mandelshtam and H. S. Taylor, A simple recursion polynomial expansion of the Green's function with absorbing boundary conditions. Application to reactive scattering, *J. Chem. Phys.* **103**, 2903 (1995).
8. U. Peskin, W. H. Miller, and Å. Edlund, Quantum time-evolution in time-dependent fields and time-independent reactive-scattering calculations via an efficient Fourier grid preconditioner, *J. Chem. Phys.* **103**, 10030 (1995).
9. Y. H. Huang, D. J. Kouri, and D. K. Hoffman, A general, energy-separable polynomial representation of the time-independent full Green operator with applications to time-independent wavepacket forms of Schrödinger and Lippmann-Schwinger equations, *Chem. Phys. Lett.* **225**, 37 (1994).
10. J. D. Gezelter and W. H. Miller, Resonant features in the energy dependence of the rate of ketene isomerization, *J. Chem. Phys.* **103**, 7868 (1995).
11. U. Peskin and W. H. Miller, Reactive scattering theory for field induced transition, *J. Chem. Phys.* **102**, 4084 (1995).
12. U. Manthe and W. H. Miller, The cumulative reaction probability as an eigenvalue problem, *J. Chem. Phys.* **99**, 3411 (1993).

13. S. M. Auerbach and C. Leforestier, A new computational algorithm for Greens functions - Fourier transform of the Newton polynomial expansion, *Comput. Phys. Commun.* **78**, 55 (1993).
14. I. Vorobeichik, N. Moiseyev, D. Neuhauser, M. Orenstein, and U. Peskin, Calculation of light distribution in optical devices by a global solution of an inhomogeneous scalar wave equation. [IEEE J. Quant. Elec., submitted]
15. J. J. Sakurai, *Modern Quantum Mechanics* (Addison-Wesley, Menlo Park, CA 1985).
16. J. R. Taylor, *Scattering Theory* (Wiley, New York, 1972).
17. R. S. Varga, *Matrix Iterative Analysis* (Prentice Hall, Englewood Cliffs, NJ, 1962).
18. L. A. Hageman and D. M. Young, *Applied Iterative Methods*, (Academic Press, New York, 1981).
19. Y. Saad, *Iterative methods for sparse linear systems* (PWS, Boston, 1996).
20. R. Barret, M. Berry, T. Chan, J. Demmel, J. Donato, J. Dongarra, V. Eijkhout, R. Pozo, C. Romine, and H. van der Vorst, *Templates for the Solution of Linear Systems: Building Blocks for Iterative Methods* (Soc. Indus.-Appl. Math., Philadelphia 1993).
21. R. W. Freund, G. H. Golub and N. Nachtigal, Iterative Solution of linear systems, *Acta Numer.* 1 (1992).
22. Y. Saad and M. H. Schultz, GMRES: A generalized minimal residual algorithm for solving nonsymmetric linear systems, *SIAM J. Sci. Stat. Comput.* **7**, 856 (1986).
23. R. W. Freund and N. Nachtigal, QMR—A quasi-minimal residual method for non-Hermitian linear systems, *Numer. Math.* **60**, 315 (1991).
24. R. W. Freund and N. Nachtigal, *QMRPAC and Applications*, ORNL Technical Report ORNL/TM-12753, (1994). [QMRPACK—A package of QMR algorithms, *ACM Trans. Math. Software* **22**, 46 (1996)]
25. R. Kosloff, Quantum molecular dynamics on grids, in *Dynamics of Molecules and Chemical Reactions* (edited by J. Zang and R. E. Wyatt (Dekker, New York, 1995).
26. R. Kosloff, in *Numerical Grid Methods and Their Application to Schrödinger's Equation*, NATO ASI Series C 412, edited by C. Cerjan (Kluwer Academic, Amsterdam, 1993).
27. R. Kosloff, Propagation methods for quantum molecular dynamics, *Ann. Rev. Phys. Chem.* **45**, 145 (1994).
28. D. T. Colbert and W. H. Miller, A novel discrete variable representation for quantum mechanical reactive scattering via the S-matrix Kohn method, *J. Chem. Phys.* **96**, 1982 (1992).
29. R. P. Ratowsky, J. A. Fleck, Jr., and M. D. Feit, *Opt. Soc. Am. A.* **9**, 265 (1992).